

Real-Time Multipath Calibration of a GPS-Based Heading Reference System

Luis Serrano^{1,2}, Don Kim¹ and Richard B. Langley¹

¹*Department of Geodesy and Geomatics Engineering
University of New Brunswick, Canada*

²*Leica Geosystems AG, Heerbrugg, Switzerland*

BIOGRAPHIES

Luis Serrano holds a diploma in engineering (University of Lisbon, Portugal) and is a Ph.D. candidate at the University of New Brunswick (UNB), Canada. He carries out research in real-time precise navigation in urban environments, dealing with issues such as carrier-phase multipath mitigation, precise platform dynamics and attitude determination. Currently he works as a GNSS engineer at Leica-Geosystems AG, Switzerland, in the area of GNSS-RTK.

Don Kim is a senior research associate in the Department of Geodesy and Geomatics Engineering at UNB. He has a Bachelor's degree in urban engineering and an M.Sc.E. and Ph.D. in geomatics from Seoul National University. He has been involved in GPS research since 1991 and active in the development of ultrahigh-performance RTK systems. He received the Dr. Samuel M. Burka Award for 2003 from The Institute of Navigation (ION).

Richard B. Langley is a professor in the Department of Geodesy and Geomatics Engineering at UNB, where he has been teaching and conducting research since 1981. He has a B.Sc. in applied physics from the University of Waterloo and a Ph.D. in experimental space science from York University, Toronto. Professor Langley has been active in the development of GPS error models since the early 1980s and is a contributing editor and columnist for GPS World magazine. He is a fellow of the ION and shared the 2003 ION Burka Award with Don Kim.

ABSTRACT

Differential carrier-phase GPS-based attitude determination represents an attractive alternative to expensive and complex inertial measurement units (IMUs) and attitude heading reference systems (AHRS), for aeronautical, marine and machine-guidance applications. Previous work in GPS-based attitude

systems, using ultra-short baselines (less than a couple of metres) between three/four antennas, have been shown to provide high accuracies, most of the time to the sub-degree level in yaw, pitch and roll.

However, using three/four antennas might be still a complex approach due to all the hardware involved, especially if the receivers are equipped with heavy and expensive multipath-mitigation devised antennas. Clearly multipath is one of the most limiting factors in accuracy and reliability regarding GPS-based attitude systems, as even a small separation between the antennas causes different and highly decorrelated phase-multipath errors.

At present, there are in the market low-cost single-frequency (or dual-frequency) receivers which are relatively cheap and weigh less than a kilogram (including the antenna, engine, interface board, power supply, cables) and therefore do not represent a problem for any kinematic platform to carry just two receivers. With two antennas it is possible to determine yaw and pitch angles, which for some applications is sufficient (such as for precision agriculture), and depending on their placement in the platform body, make the determination of these two angles quite robust.

At UNB we have been developing carrier-phase multipath-mitigation procedures for kinematic applications, using single-difference multipath observables with a dual-antenna system. These observables are obtained from the higher-order range-dynamic observations coming from the two antenna pseudo-random motions in kinematic applications, and thus originate a system independent of the platform/antenna chosen. In this paper, we describe how the higher-order range-dynamics observations, such as range-rates and range-accelerations, can be devised to be immune to multipath, and therefore how they can be optimally used to clean the carrier-phase observable used to estimate two of the attitude angles.

Furthermore, in place of comparing the results from this study with the output of accelerometers or gyroscopes (hence having to take care of their annoying systematic errors/biases), we compare the results instead with “truth” platform-dynamic information from a GNSS hardware-simulator.

INTRODUCTION

If the relative position of two antennas can be determined with a sub-centimetre accuracy using the carrier phase observable, two of the three attitude parameters, usually heading and pitch angles of the platform can be estimated.

Suppose that the baseline is mounted along the longitudinal direction (body-fixed x-axis), then the baseline vector in the body frame is [Fan *et al.*, 2005]:

$$R_b = [b \ 0 \ 0]^T$$

where b is the length of the baseline. The estimated baseline vector in the local level system is:

$$R_n = [x_n \ y_n \ z_n]^T$$

Then the heading and pitch angles can be calculated using:

$$\psi = \tan^{-1} \left(\frac{x_n}{y_n} \right) \quad (1)$$

$$\phi = -\tan^{-1} \left(\frac{z_n}{\sqrt{x_n^2 + y_n^2}} \right) \quad (2)$$

Therefore this paper focuses on an approach to calibrate or ameliorate the carrier-phase multipath before one actually fixes the integer ambiguities thus allowing one to estimate precisely two of the Euler angles. This makes this technique very interesting as it does not depend on a fixed solution as many other methods do. Hence, some explanation will be given about the other multipath methods, and the one proposed.

There are currently mainly three methods to mitigate, or at least ameliorate, the carrier-phase multipath error effect on precise (in real-time or post-processing) GNSS applications:

1. Receiver and antenna robust design against the multipath spectra (to the highest possible extent);

2. Careful selection of site or location on a platform of the antenna(s), in order to avoid to a maximal extent the multipath effect;
3. Carrier-phase multipath processing (dedicated algorithms);

The first method requires specific hardware design (with an emphasis on the research level and allocation of resources) and historically has been quite successful tackling most of the multipath errors, especially on the code observable.

The second method is the simplest and most cost-effective. However, it is very limited in terms of applicability, especially when the site scenario changes rapidly as is the case in kinematic applications.

The last method is the one chosen by the authors in tackling the carrier-phase multipath problem for several reasons: firstly, it does not require a big investment in the receiver/antenna design part (which for many companies is certainly a plus); secondly, it can be easily adapted to several applications (since it is mainly dependent on the software side); and finally, it is independent of the hardware chosen (of course, with some adaptation in the software).

It certainly also has a few negative aspects. For example, the filtering of multipath will always have some time-latency in order to process the actual epoch of data being used. However, since most of the RTK applications use a high data rate of up to 20 Hz, this may not be a real problem. Besides, the more problematic low-frequency multipath has periods stretching from a few minutes to tens of minutes.

In our approach we use a pair of antennas, connected to the same oscillator (to remove the common receiver clock bias), and distanced between each other sufficiently, but close enough to sense the same effective reflector.

This method, which is thoroughly described in two previous papers from the same authors (see Serrano *et al.* [2005] for more details), was developed having in mind the idea to obtain an observable which would physically mimic or represent the between-antenna multipath effect. Once this observable is found, its parameterization is based on the geometric parameters between the antennas and reflector(s). Therefore, the multipath effect at each antenna is recovered and its effect is corrected at each antenna.

Since it is almost impossible to obtain and separate a multipath observable for just one antenna, especially in near real-time scenarios, the two antenna system would incorporate the advantages of eliminating most of the

common biases to both antennas, while still keeping a clear and distinct multipath signature.

This advantage is certainly a necessary condition in this study, and comes from the fact that carrier-phase multipath errors, unlike other biases, are not eliminated after differencing the measurements obtained from two close-by antennas. Furthermore, this fact can be accurately explained by the theory of uniform plane wave fields.

UNIFORM PLANE WAVE FIELDS

From the definition of a uniform plane wave, we note that such a wave not only is locally plane (i.e., it has \mathbf{B} , \mathbf{E} and $\hat{\mathbf{s}}$ everywhere spatially orthogonal to each other, where \mathbf{B} is the magnetic field, \mathbf{E} the electric field, and $\hat{\mathbf{s}}$ is the unit direction vector), but truly plane [McNamara *et al.*, 1990].

Uniform plane waves are the workhorse of engineering scattering problems due to the ease in defining trajectories for ray path tracing (which allows the study of polarization, as well as the variation of amplitude and phase along the ray path).

And even though truly plane waves are an ideal abstraction, for our purposes and having in mind that the antennas are usually located in such a small distance from each other, then one can consider it a valid abstraction.

In practice, launching a single ray is not possible; however one can work with a selected axial ray plus an infinite number of rays surrounding it. Because the vectors $\hat{\mathbf{s}}$ are perpendicular to surfaces of constant phase (equiphase surfaces), the rays defined earlier are normal to these surfaces. Therefore, \mathbf{B} , \mathbf{E} and $\hat{\mathbf{s}}$ are mutually perpendicular at any point on a ray, and there are no field components in the propagation direction.

The ray picture of such a uniform wave is shown in the next picture (Fig. 1), with all rays normal to the equiphase surfaces. It emphasizes the fact that, as far as ray representation is concerned, such a uniform plane wave consists of infinitely many parallel rays propagating in direction $\hat{\mathbf{s}}$.

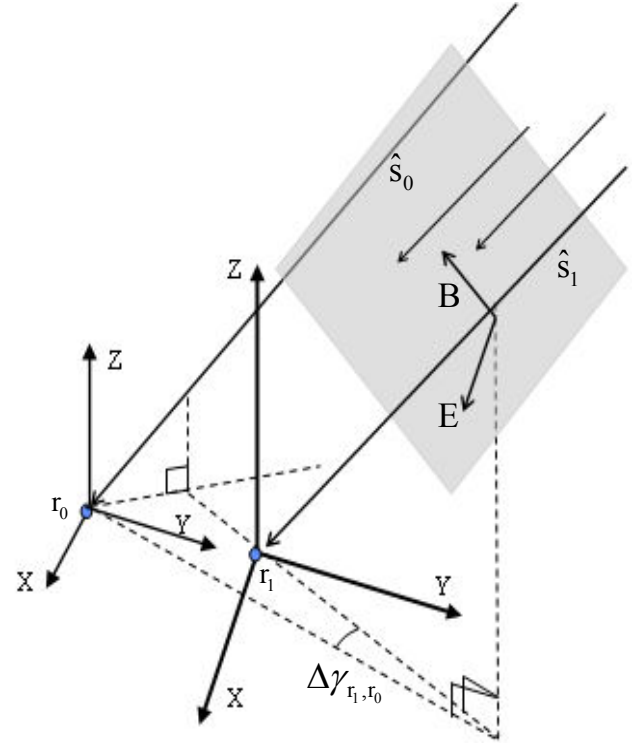


Figure 1: Geometric view of a uniform plane wave field with two antennas close to each other (r_0 and r_1 are the three-dimensional phase-center coordinates of master and slave antenna, respectively).

In our study, these relationships are very important due to the fact that we are considering the multipath errors arising from smooth, almost perfect reflectors, which cause the most serious multipath spectra (specular), especially when the reflector is located within a short distance of the antenna(s).

Any change in the relative position between antennas most likely will affect at a small scale the amplitude and polarization of the signals reflected and sensed by the two antennas (depending on their distance). However, the phase will definitely change significantly along the ray trajectory between the plane waves passing through each of the antennas. This can be seen in the equation which describes the single-difference multipath between two close antennas (see Ray *et al.* [1998] and Serrano *et al.* [2005] for further discussion):

$$\Delta M_{0,1} = M_0 - M_1 = \arctan \left(\frac{a_1 \sin \gamma_{r_1} - a_0 \sin \gamma_{r_0} + a_{r_1} a_{r_0} \sin(\gamma_{r_1} - \gamma_{r_0})}{1 + a_1 \cos \gamma_{r_1} + a_0 \cos \gamma_{r_0} + a_{r_1} a_{r_0} \cos(\gamma_{r_1} - \gamma_{r_0})} \right) \quad (3)$$

where the angle $\gamma_{r_1} - \gamma_{r_0} = \Delta \gamma_{r_1, r_0}$ (depicted in Fig. 2) is the relative multipath phase-delay between the antennas and a close effective reflector (a_0 and a_1 are the multipath

signal amplitudes in master and slave antennas respectively, and are dependent on the reflector characteristics - reflection coefficient - and receiver tracking-loop).

Having this important concept in mind, which represents the physical foundation of the current study, one can define the steps involved in our strategy to mitigate (or ameliorate) the multipath effect.

MIMICS STRATEGY

As this study is based on an objective to mimic as much as possible the multipath effect from effective reflectors in kinematic scenarios with variable dynamics we decided to name the strategy **MIMICS** (Multipath Profile from Between ReceIvers DynAMICS).

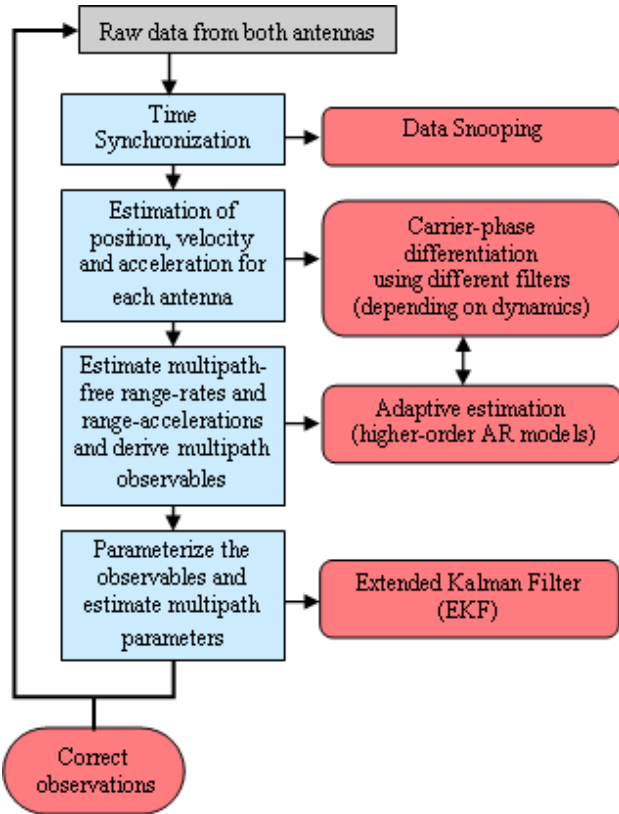


Figure 2: Steps involved in the **MIMICS** strategy.

Starting with the first step, data from both receivers are collected and synchronized. An external oscillator is used to supply the same frequency to both receivers in order to eliminate, through differencing, the common receiver-clock biases (Fig. 3).

This step also involves data quality control due to the fact that outliers are very common, where the most important are due to cycle-slips. Since the multipath observables are developed based on data time-filtering, it is essential

to detect any nonconformity between measurements from the two receivers that could lead to erroneous multipath estimates.

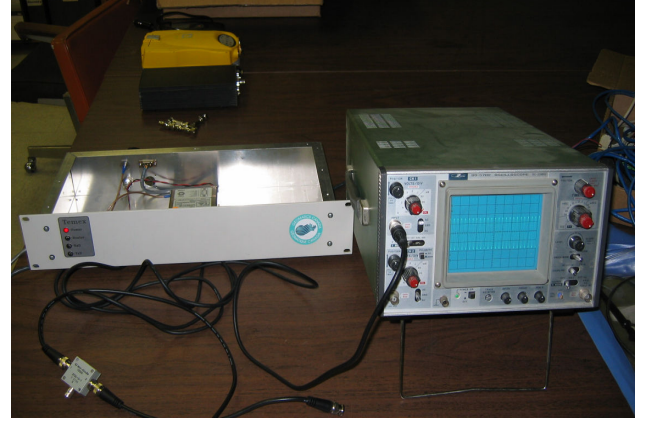


Figure 3: Temex LPFRS-01/5M external oscillator used in our studies, connected to an oscilloscope.

In the second step an approximate position for both antennas is necessary, but can be relaxed to a few meters using a standard code solution. This highlights the fact that one does not need to fix the ambiguities in order to fix multipath on carrier-phase, as is done in other approaches.

However, a very precise estimation of both antenna velocity and acceleration (in real time) is carried out using the carrier-phase observable. Not only the antenna velocity and acceleration estimates should be very precise (on the order of a few mm/s, and mm/s² respectively) but also immune to low-frequency multipath signatures. This is another necessary condition in our approach, as we use the antennas' multipath-free dynamic information to separate multipath from raw data.

This is seen in the next equation where the differenced-in-time single-difference multipath measurement is given:

$$\delta\Delta M_{m,s}^{prn}(t_k, t_{k-\tilde{\alpha}}) \approx \delta\Delta\Phi_{m,s}^{prn}(t_k, t_{k-\tilde{\alpha}}) - \delta\Delta r_{m,s}^{prn}(t_k, t_{k-\tilde{\alpha}}) - \delta\Delta\varepsilon_{m,s}^{prn}(t_k, t_{k-\tilde{\alpha}}) \quad (4)$$

where

$$\delta\Delta r_{m,s}^{prn}(t_k, t_{k-\tilde{\alpha}}) = \Delta\dot{r}_{m,s}^{prn}(t_{k-\tilde{\alpha}}) + \dots + \frac{\partial^n \Delta r_{m,s}^{prn}}{\partial t^n}(t_{k-\tilde{\alpha}}) \frac{\tilde{\alpha}^n}{n!} \quad (5)$$

Taking an ensemble of data representing the left-hand side of equation 2 (where its length can vary between a few seconds to a couple of minutes depending on whether the platform is in static or kinematic mode):

$$E\left\{\int \delta\Delta M_{m,s}^{prn}(t_k, t_{k-\bar{\alpha}})\right\} \approx$$

$$E\left\{\int \delta\Delta M_{m,s}^{prn}(t_k, t_{k-1})\right\} - E\left\{\int \delta\Delta M_{m,s}^{prn}(t_{k-\bar{\alpha}})\right\} = -\Delta M_{m,s}^{prn}(t_{k-\bar{\alpha}}) \quad (6)$$

where E is the expected value operator. The first term on the left side of the equation goes to zero and the second term is the expected value of a constant (which is a constant itself).

This is another topic covered in the papers described before, nevertheless it is important to give an overview about its implementation, especially concerning the development of the filters used as they play a big role in this approach.

DIGITAL DIFFERENTIATORS

There are important classes of FIR (Finite Impulse Response) differentiators which are highly accurate at low frequencies. It was demonstrated that the coefficients of the maximally linear digital differentiator of order $2N+1$ are the same as the coefficients of a central difference approximation of order N [Khan and Ohba, 1999], which are used in our approach to derive higher-order ($\dot{\Phi}, \ddot{\Phi}, \ddot{\ddot{\Phi}}, \dots$) range dynamics from the carrier-phase observable [Serrano *et al.*, 2004]. For example, the tap coefficients d_k^p for a second-order differentiator used to obtain range accelerations are given by:

$$d_k^{(2)} = \frac{2!(-1)^{k+1} N!^2}{k^2(N-k)!(N+k)!}, \quad k = \pm 1, \dots, \pm N \quad (7)$$

$$d_0^{(2)} = -2 \sum_{k=1}^N d_k^{(2)}. \quad (8)$$

Therefore, the central difference approximation of the second-order derivative for the arbitrary order of $2N$ can be written as:

$$f_i^{(2)} = \frac{1}{T} \sum_{k=-N}^N d_k f_{k+i}, \quad (9)$$

where T is the data sample interval. Another advantage of this class is that within a certain maximum allowable ripple on amplitude response of the resultant differentiator, its pass band can be dramatically increased. In our approach this is something fundamental as the multipath in kinematic scenarios is conceptually treated as high-frequency correlated multipath, depending on the platform dynamics and the reflector(s) distance.

The derivation of these filters has the two-fold advantage of eliminating the low-frequency multipath component in the precise derivation of higher-order range-dynamics, while at the same time allowing accurate estimates at high-frequencies due to the wider pass-band. Therefore, it can be considered a band-pass filter.

From the computational point of view it is also advantageous: In real-time it becomes easier to derive these coefficients adaptively depending on the platform velocity and acceleration.

ADAPTIVE ESTIMATION USING HIGHER-ORDER AR (AUTO-REGRESSIVE) MODELS

Using equation 4 again, and focusing only on the first term on the left side of the equation:

$$E\left\{\int \delta\Delta M_{m,s}^{prn}(t_k, t_{k-1})\right\} \quad (10)$$

it is equal to zero only if all the terms involved in the integration behave truly as a stochastic process. From the beginning of this study it became clear that estimation of multipath in a kinematic scenario has to be understood as the estimation of time-correlated random errors. However there is not a straight-forward way to find the correlation periods and model the errors. In fact, even when using the time difference of multipath between antennas nothing guarantees that its expected value goes towards zero.

Basically the idea is to decorrelate the between-antenna relative multipath through the introduction of a pseudo-random motion. As one cannot completely rely only on a decorrelation through mechanical motions, one also has to do it through the mathematical “whitening” of time-series.

Nevertheless, the ensemble of data depicted in the above formulation can be modeled as an oscillatory random process, for which second or higher order auto-regressive (AR) models can provide more realistic modeling in kinematic scenarios.

An autoregressive process is one represented by a difference equation of the form:

$$X(n) = \sum_{i=1}^p \theta_{p,i} X(n-i) + e(n) \quad (11)$$

where $X(n)$ is the real random sequence, $\theta_{p,i}$ where $i = 1, \dots, p$, and $\theta_{p,p} \neq 0$ are parameters, and $e(n)$ is a sequence of independent and identically distributed zero-mean Gaussian random variables, that is:

$$E\{e(n)\} = 0$$

$$E\{e(n)e(j)\} = \begin{cases} \sigma_n^2, & n = j \\ 0, & n \neq j \end{cases} \quad (12)$$

The sequence $e(n)$ is called white Gaussian noise. Thus an autoregressive process is simply another name for a linear difference equation model where the input or forcing function is white Gaussian noise [Shanmugan and Breipohl, 1988].

Equation 11 can be easily reduced to a state model of the form:

$$X(n) = \Theta X(n-1) + E(n) \quad (13)$$

which is more easily applied to real-time processing algorithms. The AR coefficients can be obtained through:

$$r_{XX} = R\Theta \quad (14)$$

where R is the correlation coefficient matrix, r_{XX} is the correlation coefficient vector, and Θ is the autoregressive coefficient vector. This matrix equation is called the Yule-Walker equation. Because R is invertible, we can obtain:

$$\Theta = R^{-1}r_{XX} \quad (15)$$

Therefore the last equation can be used to estimate the parameters $\theta_{p,i}$ of the model from the estimated values of the correlation coefficient $r_{XX}(k)$, and in general:

$$\begin{bmatrix} r_{XX}(1) \\ r_{XX}(2) \\ \vdots \\ r_{XX}(p) \end{bmatrix} = \begin{bmatrix} 1 & r_{XX}(1) & r_{XX}(2) & \cdots & r_{XX}(p-1) \\ r_{XX}(1) & 1 & r_{XX}(1) & \cdots & r_{XX}(p-2) \\ \vdots & \vdots & \vdots & \vdots & \vdots \\ r_{XX}(p-1) & \cdots & \cdots & \cdots & 1 \end{bmatrix} \begin{bmatrix} \theta_{p,1} \\ \theta_{p,2} \\ \vdots \\ \theta_{p,p} \end{bmatrix} \quad (16)$$

Since the order of the coefficients estimation depends on the multipath spectra (dependent on the platform dynamics and reflector distance), we used a cost function to estimate in real-time the proper order.

The order was set to vary between one (a Gauss-Markov model) and five. For instance, in the case when $p = 2$ (second-order autoregressive model), $X(n)$ is given by:

$$X(n) = \theta_{2,1}X(n-1) + \theta_{2,2}X(n-2) + e(n) \quad (17)$$

$$\text{where } \theta_{2,1} = \frac{r_{XX}(1)[r_{XX}(0) - r_{XX}(2)]}{[r_{XX}(0)]^2 - [r_{XX}(1)]^2} \quad (18)$$

$$\text{and } \theta_{2,2} = \frac{r_{XX}(0)r_{XX}(2) - [r_{XX}(2)]^2}{[r_{XX}(0)]^2 - [r_{XX}(1)]^2} \quad (19)$$

The cost function uses the residual sum of squared error, which can be used to estimate σ^2 , that is:

$$\sigma^2 = \frac{1}{N-4} \left\{ \sum_{j=3}^N [X(j) - \hat{\theta}_{2,1}X(j-1) - \hat{\theta}_{2,2}X(j-2)]^2 \right\} \quad (20)$$

The order estimation which gives the lowest error is the one chosen, and this task is done iteratively until it reaches a minimum threshold value. Once this stage is fulfilled (which nevertheless requires several computations), the multipath observable can be easily obtained.

The next task would be the multipath-parameters estimation using an extended Kalman filter (EKF), according to the **MIMICS** strategy. However, at this point and for this paper we will focus on the assessment and validation of the between-receiver multipath observable, since for the first time we could clearly validate the results with a hardware simulator. The remaining part of the multipath parameters estimation and mitigation will be assessed in a following publication.

TESTS PERFORMED

The main test performed (using two NovAtel OEM4 receivers, with two pinwheel antenna GPS-600) was also meant to evaluate the amount of data necessary to perform the decorrelation, and to evaluate if the system was observable (in terms of estimating, every epoch, several multipath parameters just from two antenna observations).

In a real-life scenario one cannot afford the luxury of performing pseudo-random motions on a platform like a vehicle. However, in this scenario one has the advantage that carrier-phase embedded dynamics are changing faster and in a three-dimensional mode (antennas sense different pitch and yaw angles). Thus a faster and more robust decorrelation is possible (Fig. 4).

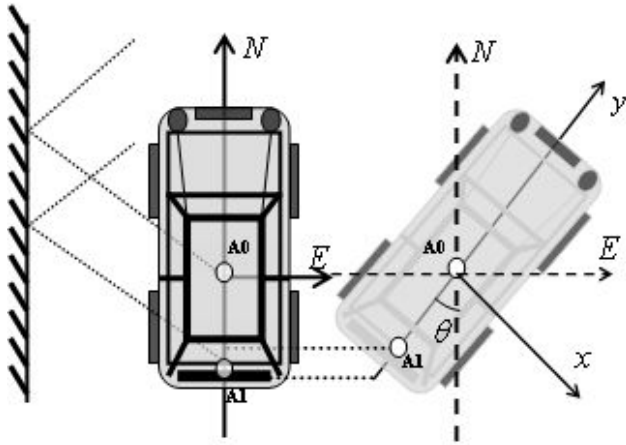


Figure 4: A schematic view of how the random motion of a vehicle creates different (and decorrelated) multipath signatures in two antennas, coming from the same effective/composed reflector(s).

In the next figure one can see the setup based on the scheme depicted in the previous figure. One can see a third antenna which was used to estimate GPS-based attitude solutions (although interesting to the multipath research, the requirement to use another receiver would just make this approach more complex).



Figure 5: Kinematic test setup (there is a huge blockage – the façade of a building with several floors - not visible in the picture, and serving as the effective reflector in the tests, because of its dimensions and smoothness of its surfaces).

The results from this test can be seen in Fig. 6. In the bottom figure one can see the kind of motion performed by the platform. Accelerations, jerk, idling, and several stops were done on purpose to see the resultant multipath spectra between the antennas. The reference station was located no more than 110m away from the vehicle antennas during the test. As such, most of the usual biases were removed from the solution and the only remaining bias can be attributed to multipath.

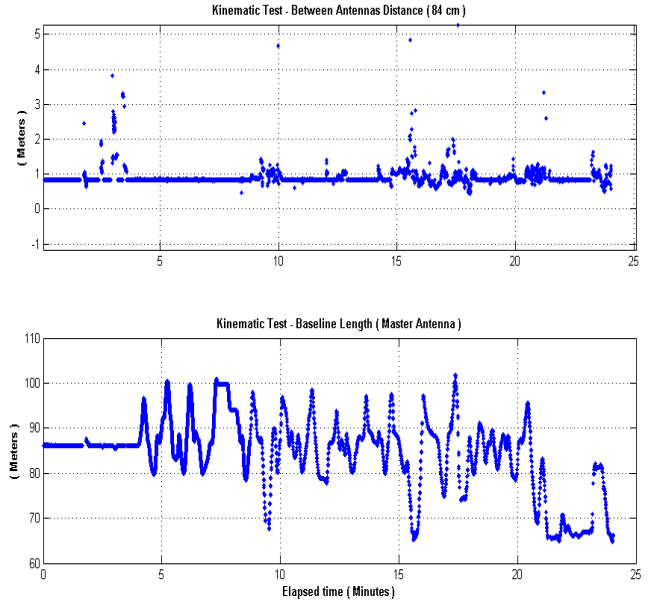


Figure 6: Results from the kinematic test

In the top figure one can see the geometric distance calculated from the fixed-solutions of both antennas. Since the bar was accurately measured before (84 cm) it is easier in this way to evaluate the solution quality. The “outliers” seen in the picture come from code solutions because the building mentioned before was blocking most of the satellites from the opposite side. As such, many times fewer than 5 satellites were available.

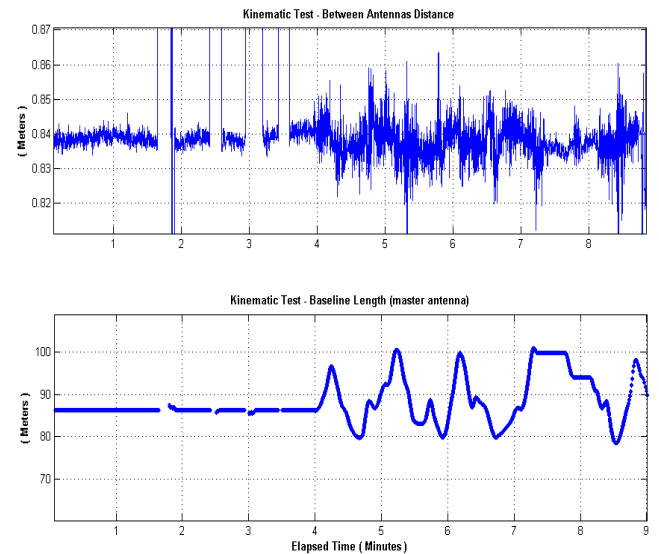


Figure 7: Zoom to the kinematic test results

Making a zoom on the first 9 minutes (Fig. 7), one can see that when the car is still stopped the multipath has a very clear quasi-sinusoidal behaviour with a period of a

few minutes. Also, one can see that it is zero meaned as expected (unlike code multipath). When the car starts moving, the noise figure is amplified (depending on the platform velocity), but one can still see a mixture of low-frequency components coming from multipath (although with shorter periods).

This proves, firstly, that regardless of the distance between two antennas multipath will not be eliminated after differencing, as with other biases. Secondly, the building façade acting as a constant smooth reflector creates the most problematic kind of multipath: the deterministic specular reflection. And thirdly, that when the platform has varied dynamics, multipath spectra will change accordingly starting from the low-frequency components towards the high-frequency (diffraction, probably also coming from the building edges and corners). As such, our approach to adaptively model multipath in real time as a quasi-random process makes sense.

The exact test scenario was implemented with the same hardware, but using data from a hardware-simulator (Spirent 4760) to validate this approach instead of real-live satellite signals.

In the next figure one can see both receivers connected to the two simulator RF outputs, and the external oscillator connected to the receivers via a splitter.



Figure 8: Hardware simulator setup with all the necessary equipment.

In Fig. 9 one can see the potential in using multipath hardware-simulated data through the use of pre-defined perfect reflectors in the vicinity of the antenna(s).

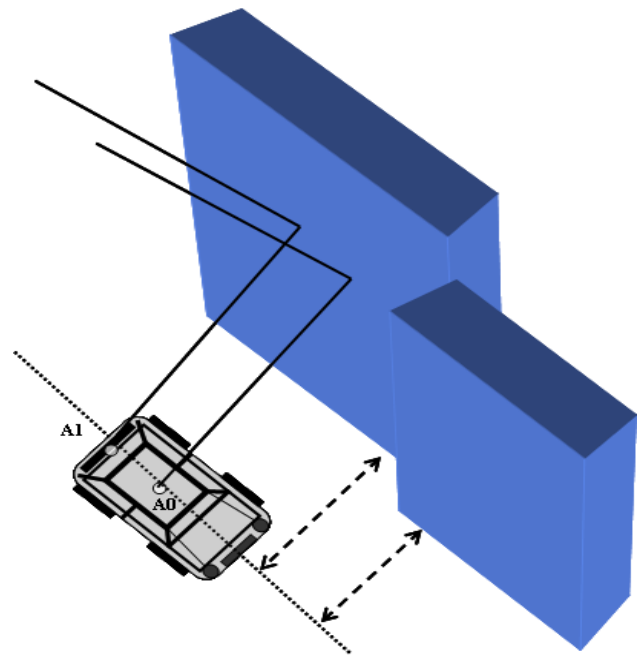


Figure 9: Illustration of one of the possible scenarios implemented in the simulator.

For each multipath path, one channel is allocated and superimposed on the direct signal. Its location (thus working as a reflector) can be defined and even pre-programmed to change its dimensions and relative offsets to the vehicle where the antennas are located, while the vehicle roves. Besides, the vehicle dynamics can also be programmed to vary accordingly (Fig. 10).

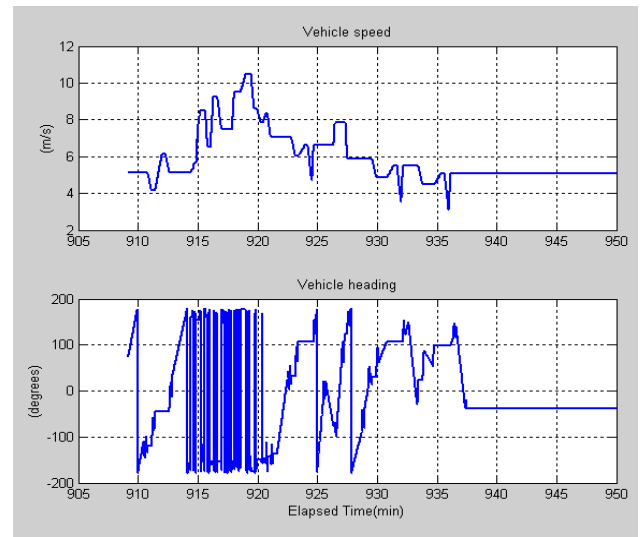


Figure 10: Vehicle speed and heading pre-programmed in the simulator scenario set-up.

TESTS RESULTS FROM THE SIMULATOR

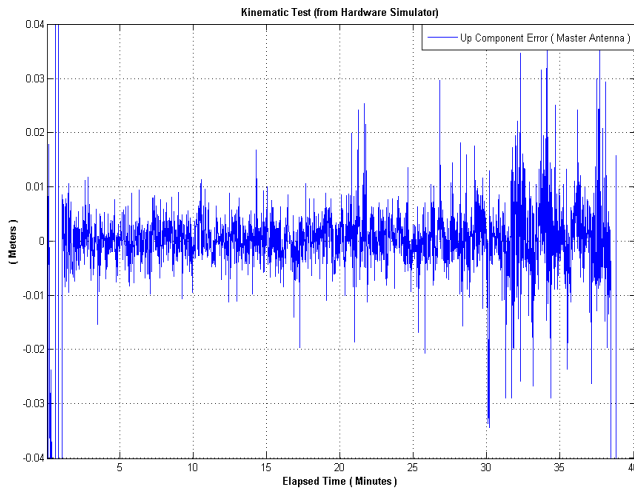


Figure 11: Comparison (in the solution domain) of the clean multipath solutions and the

Before actually seeing the results in the measurement domain, where the MIMICS approach is applied, one can see a comparison in the up component from the multipath “corrupted” solutions, and the “true” ones. Again, In the first minutes when the car is stopped the multipath sinusoidal pattern is visible, and then when the car starts moving this pattern is still visible although with shorter periods, and mixed with a considerable amplification in the noise component.

In the top panel of next figure (Fig. 12), one can see the results from the hardware-simulated data for a specific satellite (in blue). This single-difference multipath data is obtained from the difference between the described scenario with the channels-allocated reflector active, and the same test running *a posteriori* without these channels active. Besides the receiver noise, the only error source remaining after differencing should be multipath (atmospheric errors are eliminated due to the short spacing between antennas).

In the bottom panel are depicted the results using the **MIMICS** processing strategy (in red) from the data set containing the multipath.

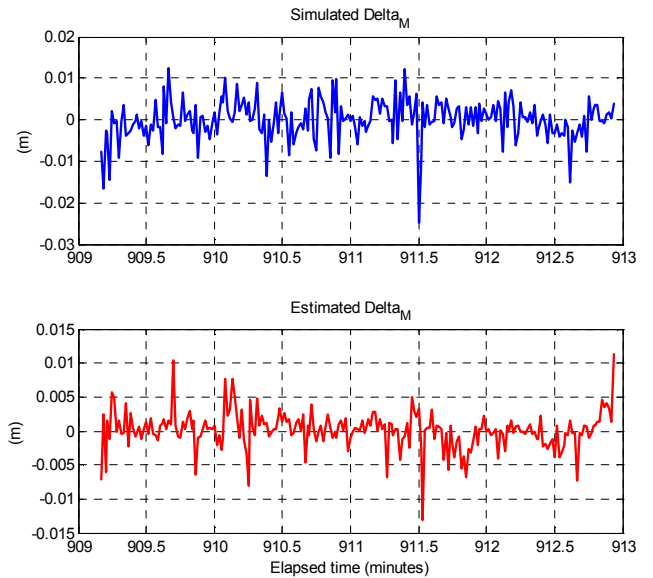


Figure 12: Test results, where in the top is the simulated multipath and in the bottom the estimated.

At first glance, it is easy to see that both plots have many similarities. However, we must acknowledge that we are not looking for exact multipath signatures since it is mostly a high-frequency multipath spectrum (thus including other noise frequency components), coming from a kinematic test.

More important is to assess if the estimated multipath amplitude and phase are related to the simulated ones. This becomes clear when one reckons that these multipath-estimated observables and the observable depicted in equation 1 are the same (therefore dependent on the multipath relative amplitude and phase).

The statistics from both plots are quite similar, where the mean value is close to zero (which confirms that carrier-phase multipath is zero-mean valued, unlike code multipath), and their amplitudes vary well within the range of $\pm 5mm$. We would expect bigger multipath values, however we used a couple of high-end receivers which already eliminate to a big extent its effect.

Since it is difficult to compare frequency components from both plots as explained before, we do the comparison in the time domain (and because we consider multipath as a highly-correlated random error with different periods).

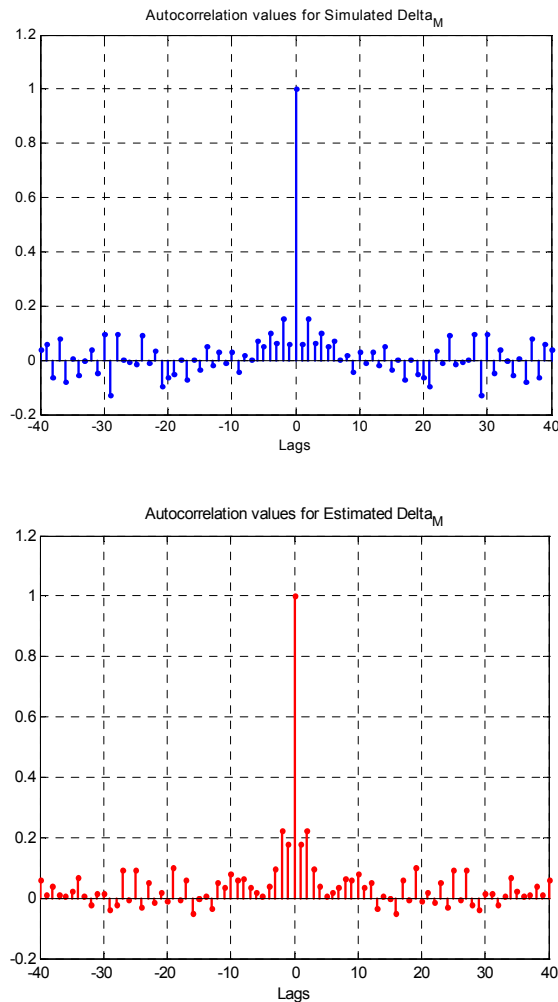


Figure 13: Autocorrelation values for simulated data (in blue) and estimated data (in red).

In Fig. 13 one can see the time-domain signals behaviour (of the simulated and estimated). It is worth noting that, in each plot, although there is clear evidence of different correlation periods, there is also a rapid decay between consecutive lags. The simulated velocity of the vehicle was programmed to vary between 0 and 40 km/h with accelerations and constant velocities (normal in an urban environment). This originated the kind of multipath we were expecting and assumed in our models, i.e., a quasi-random error depicted in the previous figure.

CONCLUDING REMARKS

We developed a novel strategy (**MIMICS**) to tackle the multipath problem in scenarios where the platform may have several antennas, variable dynamics and is surrounded by some effective reflectors (which is common in machine guidance or vehicle navigation in urban environments). Most important is the fact that this strategy is meant to be used in near real time, therefore

with some time latency, as is easily seen in Fig. 9 (dependent on data rate and on the filtering window).

From the analysis of previous figures one can say that both signals are quite random in nature (as expected) but with some parts with different correlation periods between them. Contrary to the first 5 lags where the estimated signal is more accurate, in the other lags they are somehow different, especially towards the ends of the axis. This indicates that our approach is not capturing some high-frequency components.

FURTHER RESEARCH

We will continue to improve the software part, especially in terms of the processing speed. If one wants to estimate multipath parameters synchronized with the current epoch, it is necessary to use very high data rates which can be a problem when using iterative processing algorithms as explained before.

So far, all of our tests and simulations have been designed to accurately assess and improve the mathematical background supporting the **MIMICS** strategy, and the validation of the derived multipath observables using it.

In the next steps we will definitely evaluate the impact of derived multipath observations on the position accuracy of RTK solutions, which is the overall goal.

ACKNOWLEDGMENTS

The work described in this paper was supported by the Natural Sciences and Engineering Research Council of Canada, and the Canada Foundation for Innovation and the New Brunswick Innovation Foundation.

The first author would like to thank Leica Geosystems AG, for their support.

REFERENCES

- Fan, S., K. Zhang, and F. Wu (2005). "Ambiguity Resolution in GPS-based, Low-cost Attitude Determination", *Journal of Global Positioning Systems*, Vol. 4, No. 1-2, July 2005; pp. 207-214.
- Khan, I.R. and R. Ohba (1999). "Digital Differentiators Based on Taylor Series", *IEICE Trans Fundamentals*, Vol. E82-A, No. 12, December 1999; pp. 2822-2824.
- McNamara, D.A., C.W.I. Pistorius and J.A.G. Malherbe (1990). *Introduction to the Uniform Geometrical*

Theory of Diffraction. Artech House, Norwood, MA.
471 pp.

Ray, J.K., M.E. Cannon and P. Fenton (1998).
“Mitigation of Static Carrier Phase Multipath Effects
Using Multiple Closely-Spaced Antennas”.
Proceedings of ION GPS 1998, Nashville,
Tennessee, 15-18 September 1998; pp. 1025-1034.

Serrano, L., D. Kim, and R.B. Langley (2004). “A Single
GPS Receiver as a Real-Time, Accurate Velocity
and Acceleration Sensor”. Proceedings of ION
GNSS 2004, 17th International Technical Meeting of
The Institute of Navigation, Long Beach, CA, 21-24
September 2004; pp. 2021-2034.

Serrano, L., D. Kim, and R.B. Langley (2005). “A New
Carrier-Phase Multipath Observable for GPS Real-
Time Kinematics Based on Between Receiver
Dynamics”. Proceedings of the 61st Annual Meeting
of The Institute of Navigation, Cambridge, MA, 27-
29 June 2005; pp. 1105-1115.

Shanmugan, K.S. and A.M. Breipohl (1988). *Random
Signals: Detection, Estimation and Data Analysis*.
Wiley, New York; 664 pp.